BJP British Journal of Pharmacology

DOI:10.1111/bph.12764
www.brjpharmacol.org

RESEARCH PAPER

CCDI: a new ligand that modulates mammalian type 1 ryanodine receptor (RyR1)

Chengju Tian[1]*, Chun Hong Shao[1], Christina Padanilam[1], Edward Ezell[2], Jaipaul Singh[3], Shelby Kutty[4] and Keshore R Bidasee[1,5,6]

[1]*From the Department of Pharmacology and Experimental Neuroscience,* [5]*Department of Environmental, Agricultural and Occupational Health, University of Nebraska Medical Center, Omaha, Nebraska, USA,* [2]*Eppley Institute for Research in Cancer and Allied Diseases, University of Nebraska Medical Center,* [3]*School of Forensic and Investigative Sciences, University of Central Lancashire, Preston, UK,* [4]*Joint Division of Pediatric Cardiology, University of Nebraska/Creighton University and Children's Hospital and Medical Center, Omaha, Nebraska, USA, and* [6]*Nebraska Center for Redox Biology, N146 Beadle Center, Lincoln, NE, USA*

Correspondence
Keshore R Bidasee, Department of Pharmacology and Experimental Neuroscience, 985800 Nebraska Medical Center, Durham Research Center, DRC 3047, Omaha, NE, USA. E-mail: kbidasee@unmc.edu

*Present address: Department of Neurological Sciences, College of Medicine, University of Vermont, Burlington, VT 05405.

Keywords
ryanodine receptor; sarcoplasmic reticulum, isoforms-selective, 2-cyclohexyl-3-cyclohexylimino-2,3-dihydro-pyrrolo[1,2-*c*]imidazol-1-one (CCDI)

Received
5 December 2013
Revised
21 April 2014
Accepted
29 April 2014

BACKGROUND AND PURPOSE
Ryanodine receptors (RyRs) are Ca^{2+}-release channels on the sarco(endo)plasmic reticulum that modulate a wide array of physiological functions. Three RyR isoforms are present in cells: RyR1, RyR2 and RyR3. To date, there are no reports on ligands that modulate RyR in an isoform-selective manner. Such ligands are not only valuable research tools, but could serve as intermediates for development of therapeutics.

EXPERIMENTAL APPROACH
Pyrrole-2-carboxylic acid and 1,3-dicyclohexylcarbodiimide were allowed to react in carbon tetrachloride for 24 h at low temperatures and pressures. The chemical structures of the two products isolated were elucidated using NMR spectrometry, mass spectrometry and elemental analyses. [^{3}H]-ryanodine binding, lipid bilayer and time-lapsed confocal imaging were used to determine their effects on RyR isoforms.

KEY RESULTS
The major product, 2-cyclohexyl-3-cyclohexylimino-2, 3, dihydro–pyrrolo[1,2-*c*]imidazol-1-one (CCDI) dose-dependently potentiated Ca^{2+}-dependent binding of [^{3}H]-ryanodine to RyR1, with no significant effects on [^{3}H]-ryanodine binding to RyR2 or RyR3. CCDI also reversibly increased the open probability (P_o) of RyR1 with minimal effects on RyR2 and RyR3. CCDI induced Ca^{2+} transients in C2C12 skeletal myotubes, but not in rat ventricular myocytes. This effect was blocked by pretreating cells with ryanodine. The minor product 2-cyclohexyl-pyrrolo[1,2-*c*]imidazole-1,3-dione had no effect on either [^{3}H]-ryanodine binding or P_o of RyR1, RyR2 and RyR3.

CONCLUSIONS AND IMPLICATIONS
A new ligand that preferentially modulates RyR1 was identified. In addition to being an important research tool, the pharmacophore of this small molecule could serve as a template for the synthesis of other isoform-selective modulators of RyRs.

Abbreviations
CCDI, 2-cyclohexyl-3-cyclohexylimino-2,3-dihydro-pyrrolo[1,2-*c*]imidazol-1-one; CPID, 2-cyclohexyl-pyrrolo[1,2-*c*]imidazole-1,3-dione; DCC, 1,3-dicyclohexylcarbodiimide; SR, sarcoplasmic reticulum; RyR, ryanodine receptor

Introduction

A transient rise in intracellular Ca^{2+} is used as a signal by many cells to elicit a diverse array of physiological functions including egg fertilization, hormone secretion, neurotransmitter release, muscle contraction, gene expression, cell proliferation and apoptosis (MacKrill, 1999; Berridge *et al.*, 2003). A significant percentage of this signalling Ca^{2+} is mobilized from the internal sarco(endo)plasmic reticulum (SR/ER) stores via Ca^{2+} release channels. Two classes of Ca^{2+} release channels reside on the SR/ER membranes, ryanodine receptors (RyRs) and inositol, 1,4,5-trisphosphate receptors (IP_3Rs). RyRs are significantly larger than IP_3Rs (>2.2×10^6 Da vs. ~0.8×10^6 Da) and release ~20× more Ca^{2+} from the SR/ER (MacKrill, 1999). The activities of RyRs are also tightly regulated by cytoplasmic Ca^{2+}, allowing them to serve as efficient amplification systems inside cells for executing signal transduction functions.

Three major isoforms (RyR1, RyR2 and RyR3) and several spliced variants of RyR are present in mammalian cells (Takeshima *et al.*, 1989; Otsu *et al.*, 1990; Zorzato *et al.*, 1990; Hakamata *et al.*, 1992; Futatsugi *et al.*, 1995; Giannini *et al.*, 1995; Conti *et al.*, 1996; Leeb and Brenig, 1998; Jiang *et al.*, 2003; George *et al.*, 2007). Some organs contain a predominance of one RyR isoform, for example skeletal muscles contain primarily RyR1 (Takeshima *et al.*, 1989; Zorzato *et al.*, 1990) and the heart contains mainly RyR2 (Otsu *et al.*, 1990). Other organs, like the brain, and even some cell types like smooth muscle cells, contain all three isoforms (Hakamata *et al.*, 1992; Giannini *et al.*, 1995, Neylon *et al.*, 1995). RyRs are also present in amphibians (RyR-α and RyR-β) and insects (Bull *et al.*, 1989; Lai *et al.*, 1992; Takeshima *et al.*, 1994; Cui *et al.*, 2013).

Several human diseases have also been identified that result from mutations in RyRs. The most widely studied of these are the muscle-related diseases malignant hyperthermia, central core disease, stress-induced catecholaminergic polymorphic ventricular tachycardia and arrhythmogenic right ventricular dysplasia (MacLennan and Phillips, 1992; McCarthy *et al.*, 2000; Marks *et al.*, 2002). We recently showed that alterations in the functioning of RyR2 are contributing causes for the development of a diabetic cardiomyopathy (Shao *et al.*, 2012). Others have also identified changes in function of RyRs in Alzheimer's disease (Kelliher *et al.*, 1999) and myasthenia gravis (Skeie *et al.*, 2003).

The involvement of RyR in these diseases has sparked interest in targeting these receptors for therapeutic gains. However, to the best of our knowledge, there are no reports in the scientific literature on ligands that discriminate between the RyR isoforms. The latter is especially important as a starting point when designing RyR-targeted therapeutics with minimal undesired adverse effects.

Earlier we reported that the pyrrole moiety on the triterpenoid plant alkaloid ryanodine is critical for high-affinity binding of this molecule to RyRs (Bidasee and Besch, 1998). Recent attempts in our laboratory to vary the pyrrole on a precursor molecule ryanodol using 1,3-dicyclohexylcarbodiimide (DCC) and a catalyst proved unsuccessful. However, we did notice a compound more hydrophobic than ryanodine and ryanodol that was readily formed when pyrrole-2-carboxylic acid was used as one of the reactants. Chemical investigation revealed this compound originated from an unanticipated reaction between pyrrole-2-carboxylic acid and 3-dicyclohexylcarbodiimide, under our reaction conditions. Here we describe the synthesis, structure elucidation of this new chemical entity and its effect on the activities of RyR1, RyR2 and RyR3.

Methods

Chemical synthesis

Distilled DCC (2.1 g) and pyrrole-2-carboxylic acid (PCA, 1.1 g) were dissolved in 25 mL of dried carbon tetrachloride and allowed to react for 24 h at 4°C, 20 mmHg pressure with continuous stirring. At the end of this time, distilled water (2 mL) was added, the mixture was stirred for 20 min and filtered to remove 1,3-dicyclohexyl urea. The filtrate was dried over anhydrous sodium sulfate (6 g), rotary evaporated to dryness, re-dissolved in dichloromethane (25 mL) and flashed chromatographed on silica gel (350 g), eluting with dichloromethane (1 L). A minor blue fluorescent product eluted from the column in the first 300 mL of dichloromethane. The major product eluted in the following 700 mL of dichloromethane. The latter was further purified by dissolving in dichloromethane : hexane (1:1) and leaving overnight at 4°C to precipitate.

Structural elucidation

Chemical structures of the two products isolated were elucidated from ^1H, and ^{13}C chemical shifts performed on a Varian 500 MHz NMR spectrometer (Agilent Technologies, Santa Clara, CA, USA) using tetramethyl silane (TMS) and deuterated chloroform as references. Carbon hydrogen nitrogen (CHN) elemental analyses were conducted by Midwest Micro Labs (Indianapolis, IN, USA). MS was conducted using a Thermo Finnagan LTQ mass spectrometer (Proteomic Core Facility, Indiana University, Indianapolis, IN, USA).

Preparation of SR vesicles containing RyR1

SR vesicles containing RyR1 were prepared as described previously (Tian *et al.*, 2010). Briefly, after deep anaesthesia with Inactin® (thiobutabarbital sodium, 150 mg kg^{-1} i.v., via an ear vein; Sigma-Aldrich Chemicals, St. Louis, MO, USA), fast-twitch muscles from back and hind legs were removed from male New Zealand white rabbits, placed in isolation buffer (0.3 M sucrose; 10 mM imidazole·HCl; 230 μM PMSF; 1.1 μM leupeptin, pH 7.4), homogenized (3 × 20 s, speed setting 4.5, ProScientific, Oxford, CT, USA) and centrifuged at 8,000× g_{av} for 20 min. The supernatant was discarded and the pellet was resuspended in fresh isolation buffer, homogenized a second time at speed setting 5.5 (3 × 20 s), and centrifuged at 11,000× g_{av} for 20 min. The second supernatant was filtered through cheesecloth and SR vesicles containing RyR1 were obtained by sedimentation at 85,000× g_{av} for 30 min.

Preparation of SR vesicles containing RyR2

SR membrane vesicles containing RyR2 were prepared as described previously (Tian *et al.*, 2011). After deep anaesthesia with Inactin®, hearts from 15 rats were removed and placed into ice-cold saline solution. Atrial tissues were

removed and ventricles were homogenized in a buffer consisting of 10 mM $NaHCO_3$, 230 μM PMSF, and 1.1 μM leupeptin, pH 7.4, (speed setting 4.5, Pro-Scientific, 3 × 6 s). Homogenates were centrifuged at 12,000× g_{av} for 20 min to remove nuclear and mitochondria fragments. Supernates were centrifuged at 46,000× g_{av} for 30 min and the pellet (SR membranes containing RyR2) was resuspended in buffer containing 0.25 M sucrose, 10 mM histidine, 230 μM PMSF, and 1.1 μM leupeptin, pH 7.4, quick-frozen, and stored at –80°C until used.

Preparation of ER vesicles containing RyR3

cDNA encoding rabbit RyR3 (10–15 μg, a gift from Dr. Wayne SR Chen, University of Calgary, AB, Canada) was transfected into HEK-293T cells (16 100 mm dishes of cells, 30–40% confluency grown in DMEM using the calcium phosphate method (Chen and Okayama, 1997)]. Six hours after transfection, media were replaced and cells were allowed to grow for an additional 36–44 h. Cells were then washed with 1× PBS containing 1 mM EDTA, scraped, harvested by centrifugation (500× g_{av} for 3 min), resuspended in buffer containing 0.25 M sucrose, 10 mM histidine, pH 7.3 and a protease inhibitor mix (1 mM benzamidine, 2 μg·mL^{-1} leupeptin, 2 μg·mL^{-1} pepstatin A, 2 μg·mL^{-1} aprotinin and 0.5 mM PMSF) and homogenized (3 × 6 s, speed setting 4.5, Pro-Scientific). Homogenates were centrifuged (85,000× g_{av} for 45 min) and ER membranes containing RyR3 were collected, quick frozen in liquid nitrogen, and stored at –80°C.

Preparation of junctional vesicles containing RyR1 and RyR2

Junctional membranes enriched in RyR1 were prepared by fractionating SR membranes using a discontinuous sucrose (0.8, 1.0, 1.2, 1.5 M) gradient centrifugation (103 745× g_{av} for 2 h) and collecting membranes at the 1.2–1.5 M sucrose interface (Tian *et al.*, 2010). For RyR2, junctional membranes were prepared by fractionating SR/ER membranes using discontinuous sucrose (0.6, 0.8, 1.0, 1.5 M) gradient centrifugation (103 745× g_{av} for 2 h) and collecting the membranes at the 1.0–1.2 M sucrose interface (Tian *et al.*, 2011). Membrane vesicles containing RyR3 were not fractionated using sucrose gradients.

Preparation of proteoliposomes containing RyRs

Methods for preparing proteoliposomes containing RyR1 and RyR2 are described in detail elsewhere (Tian *et al.*, 2010; 2011). For preparation of proteoliposomes containing RyR3, ER vesicles (3.0 mg·mL^{-1}) prepared from HEK-293T were solubilized with 1.5% CHAPS, instead of the usual 1.0–1.5 mg junctional membranes for RyR1 and RyR2, with the remaining purification steps identical for that of RyR1 and RyR2. Proteoliposomes were stored in the vapour phase of a liquid nitrogen freezer until used.

High-affinity [^{3}H]-ryanodine binding

[^{3}H]-Ryanodine binding assays were used to assess the ability of the compounds to interact with RyR1, RyR2 and RyR3. For this, SR(ER) membranes (0.1 mg·mL^{-1}) containing RyR1, RyR2 or RyR3 were incubated in binding buffer (500 mM KCl, 20 mM Tris-HCl, 0.3 mM $CaCl_2$, 0.1 mM EGTA, pH 7.4) containing 6.7 nM [^{3}H]-ryanodine and various amounts of the compounds (up to 200 μM) for 2 h at 37 °C. Ryanodine (1 μM) was used as a control and to determine non-specific binding. At the end of the incubation, samples were rapidly filtered through GF/C filters using a cell harvester (Brandel, Gaithersburg, MD, USA), washed three times with ice-cold binding buffer (3 mL), and the amount of [^{3}H]-ryanodine bound to the filters was quantified using liquid scintillation counting (Bidasee and Besch, 1998; Bidasee *et al.*, 2000).

For determining the effect on B_{max}, membrane vesicles containing RyR1 (0.1 mg·mL^{-1}) were incubated in binding buffer (500 mM KCl, 20 mM Tris·HCl, 0.3 mM $CaCl_2$, 0.1 mM EGTA, pH 7.4), with varying amounts of [^{3}H]-ryanodine (3.3–52.4 nM) and 50 μM of the major product for 2 h at 37°C. Non-specific binding was determined simultaneously by incubating vesicles with 1 μM unlabelled ryanodine. For determining if the ability of the reaction products to alter [^{3}H]-ryanodine binding to RyR1 was Ca^{2+}-dependent, membrane vesicles containing RyR1 (0.1 mg·mL^{-1}) were incubated in binding buffer (500 mM KCl, 20 mM Tris·HCl, 6.7 nM [^{3}H]-ryanodine, pH 7.4 and 50 μM of the major product) with varying amounts of Ca^{2+} (0–8 mM) for 2 h at 37°C. Non-specific binding was determined simultaneously by incubating vesicles with 1 μM unlabelled ryanodine.

Single channel assays

Lipid bilayer assays were used to determine the effects of the compounds on the activities of RyR1, RyR2 and RyR3. For this, phosphatidylethanolamine, phosphatidylserine and phosphatidylcholine in a ratio of 5:3:2 (35 mg·mL^{-1} of lipid) in *n*-decane were painted across the 200 μm diameter hole of a bilayer cup as described previously (Tian *et al.*, 2010; 2011; Shao *et al.*, 2012). Proteoliposomes containing purified RyR1, RyR2 or RyR3 were then incorporated into the lipid bilayer. The side of the bilayer to which proteoliposomes were added was designated as *cis*, the other side as *trans*/ground. Compounds dissolved in ethanol or DMSO were added to the *cis* chamber and vigorously stirred for ~30 s. Final ethanol or DMSO concentrations in *cis* chamber were 4%. Channel activities were then recorded for 6 min (3 min at +35 mV and 3 min at –35 mV) in symmetric KCl buffer (0.25 mM KCl, 20 mM K-HEPES, pH 7.4) with 3.3 μM Ca^{2+} in the *cis* chamber. For some experiments, recordings were obtained with varying *cis* Ca^{2+} (0.45 μM to 5 mM) in the absence and presence (80 μM) of the drugs. Drugs were added as a bolus to *cis* chamber vigorously stirred for 30–45 s before recording, and experiments were conducted at room temperature (23–25°C) in ambient oxygen. After the effect of the drug was observed, the buffer in the *cis* chamber of the bilayer apparatus where the drug was added was replaced with drug-free buffer via slow perfusion to determine if the action of the drug on the channel is reversible. Data acquisitions were performed using commercially available instruments and software (Axopatch 1D, Digidata 1322A and pClamp 10.0, Axon Instruments, Burlingame, CA, USA). Electrical signals were filtered at 2 kHz, digitized at 10 kHz, and data were analysed using pClamp (Molecular Devices, Sunnyvale, CA, USA) and Sigma Plot 10.0 (Stystat Software Inc., Chicago, IL, USA).

Effect on Ca^{2+} release from SR of C2C12 cells

Mouse skeletal muscle myoblasts (C2C12 cells) grown on laminin-coated glass-bottomed chambers in DMEM containing 1.2 mM $CaCl_2$, supplemented with 1.5% FBS and antibiotics (100 U·mL^{-1} penicillin, 100 μg·mL^{-1} streptomycin, and 100 μg·mL^{-1} gentamicin, pH 7.3) were allowed to grow and differentiate (Tian *et al.*, 2010). At 60–70% confluency, differentiated myotubes were loaded with Fluo 3-AM (5 μM, for 30 min at 37°C), washed, and placed on the stage of a laser confocal microscope (Zeiss LSM 510 equipped with an Argon-Krypton Laser, Thornwood, NJ, USA, 25 mW argon laser, 488 nm, 1% intensity; Plan-Apochromat, Thornwood, NJ, USA, 63×/1.4 oil lens, pinhole 128 μm, pixel time 1.28 μs, stack size 1024 × 1024 × 1). The compound (150 μM) was then added to the chamber and time-lapse confocal microscopy was conducted to assess changes in intracellular Ca^{2+} (every 2 s for 5 min). For some experiments, cells were treated with ryanodine (100 μM) for 5–10 min, responses measured, and then the compound of interest was added to the chamber.

Effects on Ca^{2+} from SR of rat primary ventricular myocytes

Ventricular myocytes isolated from rat hearts were attached to laminin-coated glass coverslips by incubating for 1 h at 37°C in DMEM-F12 and 1.2 mM Ca^{2+} as described previously (Shao *et al.*, 2009; 2012). Attached cells were then loaded with Fluo-3 (5 μM) for 30 min at 37°C. Extracellular Fluo-3 was removed by washing, and myocytes were placed on the stage of a laser confocal microscope (Zeiss Confocal LSM 510 confocal microscope equipped with an argon–krypton laser 25 mW argon laser, 5% intensity). The compound of interest (150 μM) was added to a corner of the chamber and changes in intracellular Ca^{2+} were assayed using time-lapse imaging. Images were taken every 2 s for 5 min. Data were analysed using Microsoft Excel (Microsoft Inc., Seattle, WA, USA) and Sigma Plot (Systat Inc., Chicago, IL, USA).

Statistical analyses

Data are expressed as means ± SEM. Statistical significance of effects was analysed using ANOVA followed by the Bonferroni *post hoc* test using Prism 5 (GraphPad Software, Inc., San Diego, CA, USA). A P value of <0.05 was taken as significant.

Chemical and reagents

[^{3}H]-Ryanodine was purchased from GE Life Sciences (Boston, MA, USA), phosphatidylserine, phosphatidylcholine and phosphatidylethanolamine were obtained from Avanti Polar Lipids Inc. (Alabaster, AL, USA). Ryanodine was isolated from the bark of *Ryania speciosa* Vahl and characterized in our laboratory as previously described (Bidasee *et al.*, 1994). All other reagents used were of the highest grade commercially available. The chemical names of the compounds synthesized and the nomenclature for RyR Ca^{2+} release channels conforms to BJP's Concise Guide to PHARMACOLOGY (Alexander *et al.*, 2013).

Results

Characterization of the products formed from the reaction of DCC and PCA

The major product isolated from the reaction between PCA and DCC exhibited R_f values of 0.25 and 0.47 in dichloromethane and dichloromethane : methanol (97:3) respectively. This compound was soluble in chloroform, dichloromethane and DMSO (20 mg·mL^{-1}), and methanol and ethanol (up to 15 mg·mL^{-1} when warmed to 50°C). Although not soluble in water, about 3–4 mg remained in solution in 1 mL of a 6:1 mixture of DMSO-distilled deionized water (warmed to 50°C). We have not tested the thermal stability of CCDI at temperatures greater than 50°C.

^{1}H NMR in deuterated chloroform with TMS as reference, revealed a quartet of triplets at δ1.23 (J = 9.5, 3.5 Hz, integrate for 1 h), another quartet of triplets at δ1.32 (J = 10.0, 3.5 Hz, integrate for 1 h) partially overlapped by a multiplet at δ1.4, (integrate for 4 h), an apparent quartet at δ1.5, (integrate for 2 h), multiplet at δ1.67, (integrate for 4 h), multiplet at δ1.84, (integrate for 6 h), quartet of doublets at δ2.34 (J = 13, 3.5 Hz, integrate for 2 h), multiplet at δ3.82 (integrate for 1 h), triplet of triplets at δ4.13 (J = 12.5, 3.5 Hz, integrate for 1 h), doublet of doublets at δ6.44 (J = 3.0, 3.5 Hz, integrate for 1 h), doublet of doublets at δ6.6 (J = 3.5, 1.0 Hz, integrate for 1 h), and doublet at δ7.18 (J = 2.5 Hz, integrate for 1 h), Supporting Information Figure S1. ^{13}C NMR revealed peaks at δ24.26, δ25.34, δ25.74, δ26.18, δ29.30, δ33.51, δ52.01, δ55.71, δ107.52, δ116.23, δ120.59, δ127.51, δ134.74, and δ159.20 (Supporting Information Figure S2). ^{13}C-attached proton test showed nine of these signals were phased with positive intensity (δ24.26, δ25.34, δ25.74, δ26.18, δ29.30, δ33.51, δ127.51, δ134.74, and δ159.20) indicating either methylene or quaternary carbons, and five phased with negative intensity (δ52.01, δ55.71, δ107.52, δ116.23 and δ120.59) indicating either methyl or methine moieties. Elemental analysis indicated 72.2% C, 14.0% N and 8.2% H and MS revealed a molecular mass of 299.06 Da. Based on these data, the major product was identified as CCDI. A mechanism for the generation of CCDI is proposed in Scheme 1. In this study, 510 mg of CCDI was obtained from the reaction of 2.1 g of DCC and 1.1 g of pyrrole-2-carboxylic acid, affording a yield of ~17%. To date, we have not isolated intermediates #1 and #2 in the reaction scheme.

The blue fluorescent compound (~10 mg) exhibited R_f values of 0.30 and 0.54 in dichloromethane and dichloromethane : methanol (97:3) respectively. Its ^{1}H NMR spectrum revealed a quartet of triplets at δ1.24 (J = 13.0, 3.0 Hz, integrate for 1 h), quartet of triplets at δ1.35 (J = 13.0, 3.0 Hz, integrate for 2 h), a multiplet at δ1.68, (integrate for 1 h), multiplet at δ 1.77, (integrate for 2 h), a multiplet at δ1.87, (integrate for 2 h), a quartet of doublets at δ2.12 (J = 13, 3.5 Hz, integrate for 2 h), a triplet of triplets multiplet at δ3.97 (J = 12.5, 4.0 Hz, integrate for 1 h), triplet t δ6.41 (J = 3.5 Hz, integrate for 1 h), doublet at δ6.74 (J = 3.5 Hz, integrate for 1 h), and doublet at δ7.21 (J = 3 Hz, integrate for 1 h), ^{13}C NMR also revealed peaks at δ25.17, δ26.18, δ30.02, δ40.57, δ51.78, δ113.14, δ117.28, δ119.87, δ125.44, and δ148.78 and δ158.84. Mass spectrometric analyses also revealed a molecular mass of 218.26 Da. Based on its mag-

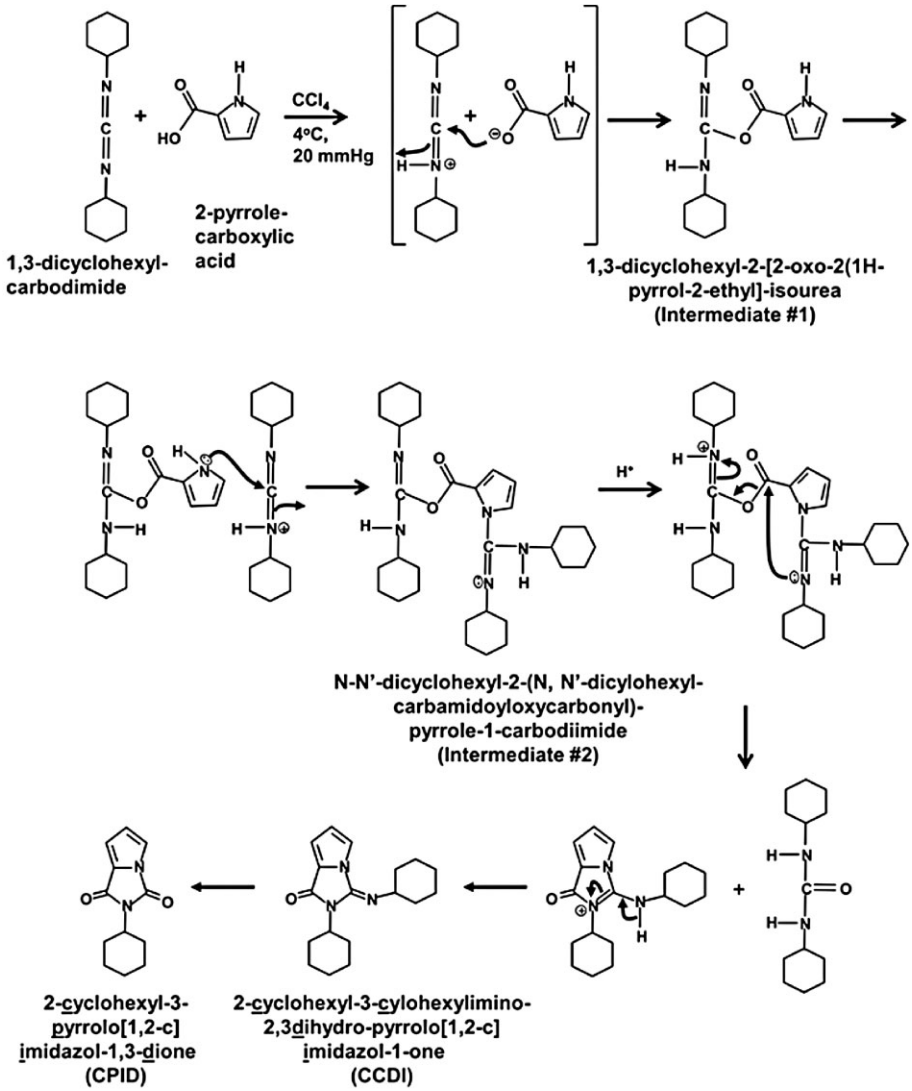

Scheme 1

Proposed reaction mechanisms for synthesis of CCDI and CPDI.

netic resonance, mass data, the fluorescent compound was identified as 2-cyclohexyl-pyrrolo[1,2-*c*]imidazole-1,3-dione (CPID). The proposed chemical structure of CPID was confirmed using X-ray crystallography (data not shown).

When CCDI was dissolved in a 6:1 mixture of DMSO/distilled deionized water and left standing at room temperature for 24 h, a small amount of CPID was formed (see Supporting Information Figure S3, thin layer chromatograph, also see Scheme 1). From these data we concluded that CPID was generated from hydrolysis/oxidation of CCDI following the addition of water at the end of the reaction. Since, the amount of CPID isolated was relatively small compared with the amount of CCDI (less than 5%), we reasoned that hydrolysis/oxidation of CCDI in water is not a rapid process.

Effects of CCDI and CPID on high-affinity binding of [^{3}H]-ryanodine to RyRs

In buffer containing 200 μM free Ca^{2+}, CCDI (0.3–200.0 μM) enhanced the binding of [^{3}H]-ryanodine to RyR1 in a dose-dependent manner. Peak enhancement of [^{3}H]-ryanodine binding occurred with 50 μM (225 ± 10% over control) and half maximum effect at 6 μM. Over the same concentration range, CCDI exhibited no significant effect on the binding of [^{3}H]-ryanodine to RyR2 or RyR3 (Figure 1B and C). CPID, the hydrolysis product of CCDI had no significant effect on the binding of [^{3}H]-ryanodine to RyR1, RyR2 and RyR3 (Figure 1).

Scatchard analysis conducted by varying the amount of [^{3}H]-ryanodine with and without 50 μM CCDI in binding buffer, revealed B_{max} values of 5.9 ± 0.4 pmol·mg^{-1} membranes and 1.9 ± 0.2 pmol·mg^{-1} membranes, respectively, (Figures 2A and B). CCDI in the binding buffer did not alter the K_d for [^{3}H]-ryanodine binding to RyR1 (4.0 ± 0.6 nM in the presence of CCDI and 4.2 ± 0.4 nM in absence of CCDI, Figure 2B).

Next we assessed if the ability of CCDI to potentiate [^{3}H]-ryanodine binding to RyR1 was dependent on the concentration of Ca^{2+} in the binding buffer. When 3.0 μM and 5.0 μM Ca^{2+} were present in the binding buffer, the amounts of [^{3}H]-ryanodine bound to RyR1, RyR2 and RyR3 were

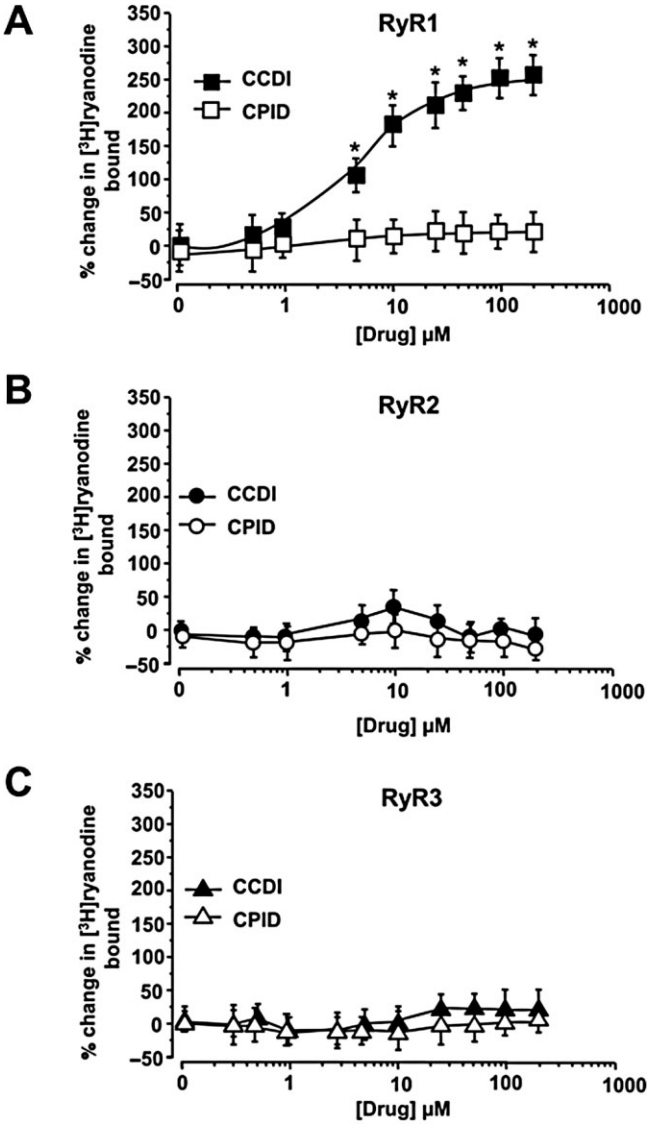

Figure 1

Effect of CCDI and CPID on the binding of [^{3}H]-ryanodine to RyR1 (A), RyR2 (B) and RyR3 (C) under optimal Ca^{2+} (200 μM free) in binding buffer. Data shown for each point represent mean ± SEM from five experiments performed using three different membrane preparations. *Denotes significantly different ($P < 0.05$) from values at 0, 0.5 and 1 μM CCDI.

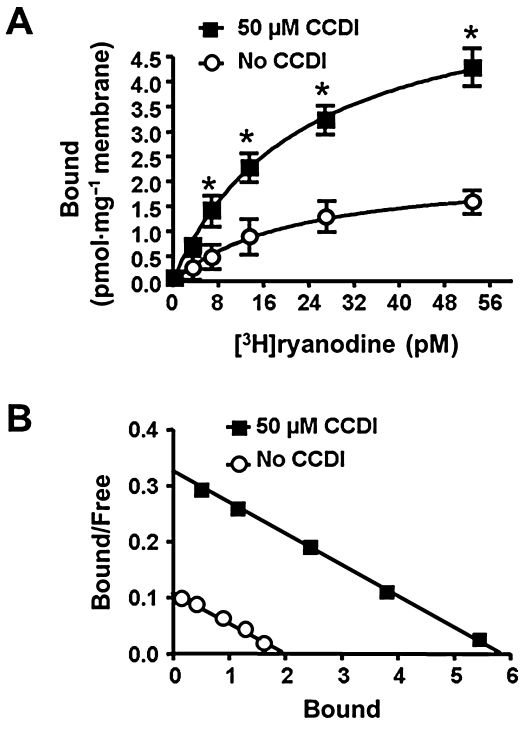

Figure 2

(A) Effect of CCDI (50 μM) on binding of varying concentrations [^{3}H]-ryanodine to RyR1 under optimal Ca^{2+} (200 μM free) in binding buffer. Data shown for each point represent mean ± SEM for five experiments performed using three different membrane preparations. (B) Scatchard (Rosenthal) analysis to assess the effect of CCDI (50 μM) on the B_{max} of [^{3}H]-ryanodine bound to RyR1 under optimal Ca^{2+} (200 μM free) in binding buffer. Data shown for each point represent mean for five experiments performed using three different membrane preparations. SEM were less than 10% and left out for clarity. *Denotes significantly different ($P < 0.05$) from values at 0, and 3.35 μM [^{3}H]-ryanodine.

negligible (≤5 fmol [^{3}H]ryanodine/100 μg membranes). Titrating the concentration of Ca^{2+} in the binding buffer upwards to 300 μM, dose-dependently increased [^{3}H]-ryanodine binding to RyRs (Figure 3), consistent with previous reports (Smith *et al.*, 1986; Emmick *et al.*, 1994). Increasing the concentration of Ca^{2+} in binding buffer beyond 300 μM also dose-dependently reduced the binding of [^{3}H]-ryanodine to RyR1, RyR2 and RyR3 (Figure 3).

Addition of CCDI (50 μM) to the binding buffer potentiated the binding of [^{3}H]-ryanodine to RyR1 at Ca^{2+} concentrations between 10 and 1000 μM, but not when Ca^{2+} concentrations in binding buffer were ≤10 or ≥1000 μM (Figure 3A). The latter are Ca^{2+} concentrations that typically promote closure of RyRs. CCDI did not significantly alter Ca^{2+}-dependent binding of [^{3}H]-ryanodine to RyR2 or RyR3 (Figures 3B and C).

Functional effects of CCDI on RyRs

Lipid bilayer assays were then used to gain mechanistic insights into how CCDI was increasing the binding of [^{3}H]-ryanodine to RyR1. When added to the *cis* chamber (equivalent to the cytoplasmic side) containing 3.3 μM Ca^{2+}, CCDI dose-dependently increased the open probability (P_o) of RyR1 at +35 mV holding potential, Figure 4A. Similar increases in P_o were also observed at –35 mV at the holding potential (data not shown). With lower concentrations of CCDI (≤80 μM), increases in the P_o of RyR1 resulted primarily from increases in the number of transitions from the closed to the opened state (Table 1). At concentrations of CCDI >100 μM, increases in P_o of RyR1 resulted also from both increases in the number of transitions from the closed to the opened state and the mean time in the opened state, (Table 1). CCDI did not alter the conductance of RyR1. Addition of CCDI to the *cis* chamber of the lipid bilayer did not significantly alter the P_o or conductance of RyR2 and RyR3 (Figure 4B and C).

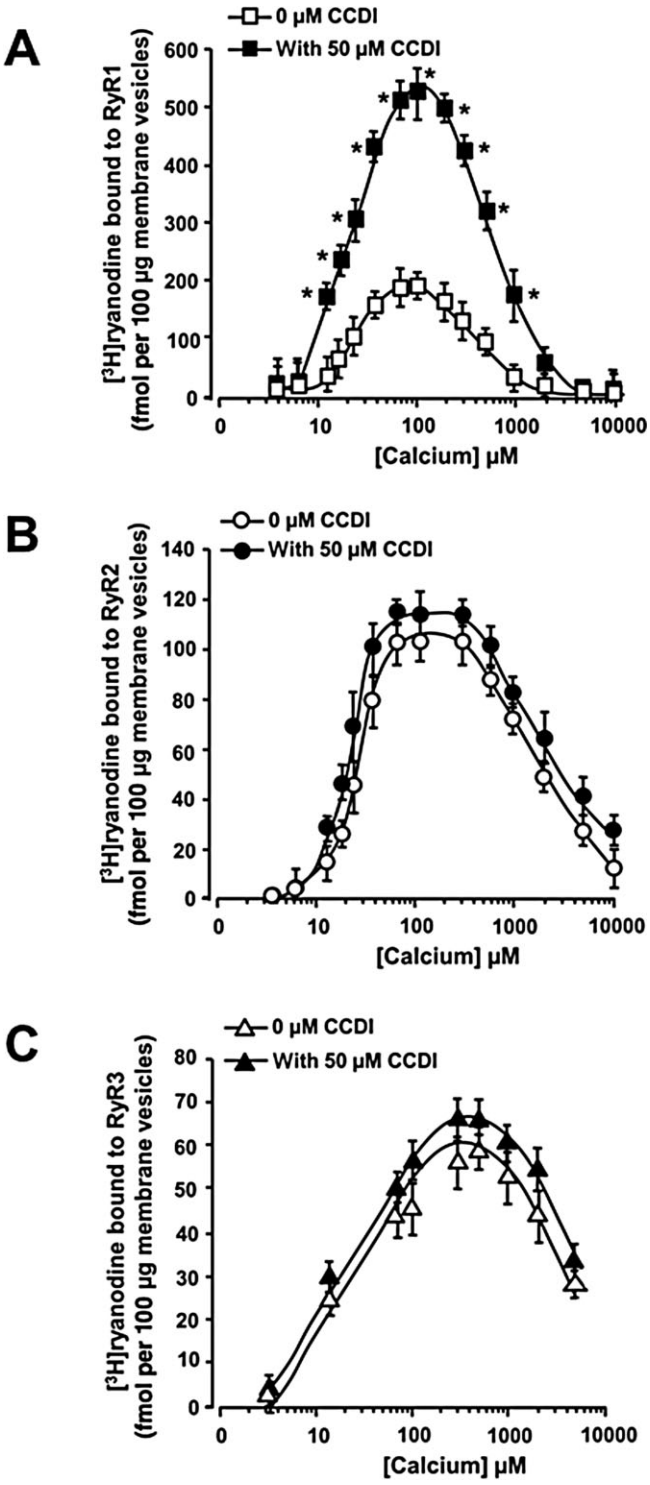

Figure 3

Effect of CCDI (50 μM) on Ca^{2+}-dependent binding of [^{3}H]-ryanodine to RyR1 (A), RyR2 (B) and RyR3 (C). Data shown for each point represent mean ± SEM for five experiments performed using three different membrane preparations. *Denotes significantly different (P < 0.05) from values at 3, 5, 1500, 3000 and 5000 μM Ca^{2+} only.

Effects of varying cis Ca^{2+} *on the responsiveness of RyR1 to CCDI*

In binding assays, CCDI did not potentiate the amount of [^{3}H]-ryanodine bound to RyR1 when the concentrations of Ca^{2+} in binding buffer were <5.0 μM Ca^{2+} and >1000 μM (Figure 3A). As these concentrations of Ca^{2+} typically promote closure of RyR1, we investigated whether the ability of CCDI to increase the P_o of RyR1 was dependent on RyR1 being in the activated (opened) state. In the presence of 0.45 μM *cis* Ca^{2+}, the mean P_o of 12 RyR1 channels studied was 0.008 ± 0.004. Increasing *cis* Ca^{2+} in a stepwise manner to 10 μM (1.0, 3.3 and 10.0 μM) dose-dependently increased the P_o of RyR1 to 0.44 [Figure 5], by increasing both the number of transitions from the closed to opened state and the dwell time in the opened state. Increasing the concentration of *cis* Ca^{2+} to 200 μM did not further increase the P_o of RyR1. Concentrations of *cis* Ca^{2+} >200 μM, dose-dependently decreased the P_o of RyR1. The highest concentration of *cis* Ca^{2+} (5000 μM) also decreased the conductance of RyR1 by 11% (from 770 ± 25 pS to 685 ± 32 pS, P < 0.05).

In the presence of 0.45 and 1.0 μM *cis* Ca^{2+}, addition of 80 μM CCDI to the *cis* chamber did not significantly alter the P_o of RyR1 [Figure 5]. At [Ca^{2+}] between 3.3 and 1000 μM, the addition of 80 μM CCDI to the *cis* chamber potentiated the P_o of RyR1, [Figure 5]. The increase in P_o was near additive with that of Ca^{2+}. At 3.3 μM *cis* Ca^{2+}, CCDI increased the Po of RyR1 by increasing the number of transitions from the closed to the opened state. Between 10 and 2000 μM, increases in P_o resulted from increases in the number of transitions from the closed to the opened state and from increases in the mean time in the opened state. With 5000 μM *cis* Ca^{2+}, CCDI did not significantly increase the P_o of RyR1.

Effects of CPID on gating and conductance of RyR1

The hydrolysis/oxidation of CCDI in water, albeit slow, prompted us to investigate the effects of CPID on the gating and conductance of RyR1. When added to the *cis* chamber containing 0.45 μM (low RyR1 activity) and 10.0 μM Ca^{2+} (high RyR1 activity), CPID did not alter the P_o of RyR1 at +35 mV holding potential, Figure 6. Varying the holding potentials from ±20 to ±60 mV also did not alter the P_o of RyR1 (data not shown). From these data we conclude that changes in P_o of RyR1 following addition of CCDI in the *cis* chamber arose solely from the actions of 'intact' CCDI and not from its hydrolysis product CPID.

Assessing the reversibility of the actions of CCDI RyR1

Next we assessed whether the effects of CCDI on RyR1 were reversible. When added to the *cis* chamber containing 3.3 μM Ca^{2+}, CCDI (80 and 160 μM) dose-dependently increased the open probability of RyR1 at ±35 mV holding potentials, Figure 7. The increase in P_o at each concentration of CCDI persisted for the duration of the experiment (6 min at each + and – 35 mV). Gently exchanging the *cis* chamber buffer (perfusion) of the lipid bilayer while stirring to remove the CCDI, attenuated the increase in P_o of RyR1 (Figure 7). In six separate occasions CCDI was re-added to the *cis* chamber, but immediately after stirring the lipid bilayer broke and we were

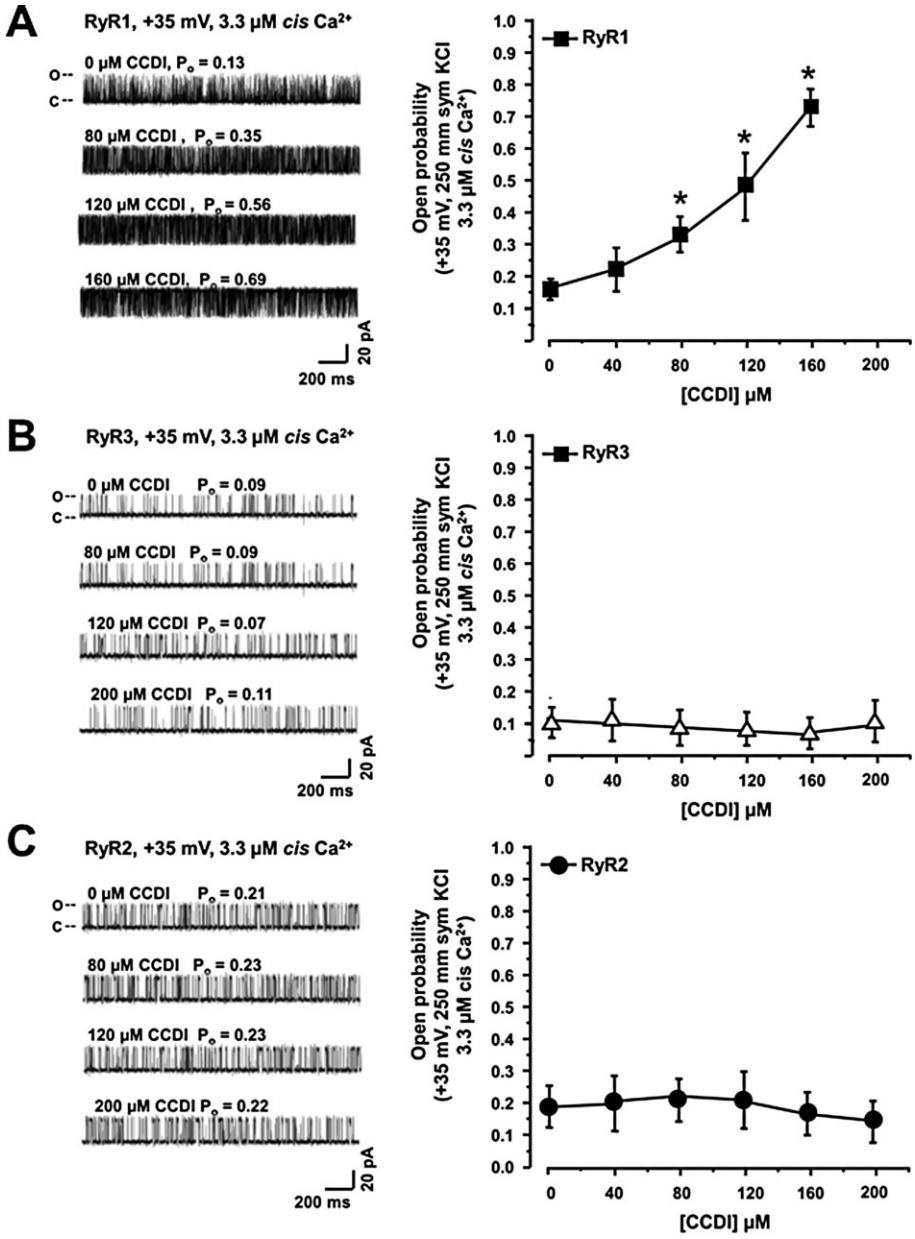

Figure 4

Effects of CCDI on open probability of RyR1, RyR2 and RyR3. (A) Left shows representative 2 s recordings of RyR1 at +35 mV in the absence and presence of increasing amounts of CCDI added to the *cis* chamber with 3.3 μM *cis* Ca^{2+} in the presence of symmetric KCl buffer solution. The graph in (A), right, shows mean ± SEM for $n = 14$ channels from two separate RyR1 preparations. *Denotes significantly different from 0 μM CCDI at $P < 0.05$. (B) Left shows representative 2 s recordings of RyR3 at +35 mV in the absence and presence of increasing amounts of CCDI added to the *cis* chamber with 3.3 μM *cis* Ca^{2+} in the presence of symmetric KCl buffer solution. The graph in (B), right, shows mean ± SEM for $n = 9$ channels from two separate RyR3 preparations. (C) Left shows representative 2 s recordings of RyR2 at +35 mV in the absence and presence of increasing amounts of CCDI added to the *cis* chamber with 3.3 μM *cis* Ca^{2+} in the presence of symmetric KCl buffer solution. The graph in (C), right: mean ± SEM for $n = 11$ channels from two separate RyR2 preparations.

unable to assess the effect of re-addition of CCDI on the P_o of RyR1.

CCDI mobilizes Ca^{2+} from internal stores of C2C12 cells

Within seconds after addition of CCDI (150 μM) to differentiated C2C12 cells in medium containing 1.2 mM Ca^{2+}, Ca^{2+} transients were observed (Figure 8A(i), also see Supporting Information Movie S1 – CCDI on C2C12 cells). Peak Ca^{2+} transient amplitude averaged over 14 cells occurred after 60–70 s [peak $\Delta F = 2.6 \pm 0.2$ fluorescence units, Figure 8B]. The Ca^{2+} transient decay time varied from cell to cell, but on average returned to basal at 190 ± 20 s after the peak amplitude [Figure 8B]. Ca^{2+} transients were also generated in

Table 1

Effect of CCDI on open probability, transitions from opened to closed states, mean time in the open state, mean time in the closed state and conductance of RyR1, RyR2 and RyR3

RyR isoform	[CCDI] (μM)	Open probability (P_o)	Number of transitions per s from closed to opened state	Mean time in the opened state (ms)	Mean time in the closed state (ms)	Conductance (pS)
RyR1(n = 16)	0	0.12 ± 0.01	254 ± 10	0.55 ± 0.21	3.55 ± 0.4	771 ± 26
	40	0.22 ± 0.04*	348 ± 14*	0.70 ± 0.31	2.31 ± 0.52*	766 ± 25
	80	0.32 ± 0.06*	506 ± 25*	0.83 ± 0.29	1.43 ± 0.39*	775 ± 30
	120	0.55 ± 0.07*	668 ± 20*	1.05 ± 0.31*	0.92 ± 0.39*	768 ± 21
	160	0.66 ± 0.07*	516 ± 15*	1.23 ± 0.31*	0.57 ± 0.32*	759 ± 32
RyR2 (n = 11)	0	0.18 ± 0.09	210 ± 17	2.44 ± 0.31	13.55 ± 4.24	732 ± 21
	40	0.22 ± 0.06	213 ± 20	2.47 ± 0.35	11.22 ± 4.70	741 ± 26
	80	0.23 ± 0.02	236 ± 20	2.50 ± 0.41	10.86 ± 3.71	736 ± 33
	120	0.24 ± 0.06	246 ± 24	2.55 ± 0.31	10.65 ± 5.91	742 ± 31
	160	0.18 ± 0.02	203 ± 15	2.36 ± 0.22	13.12 ± 6.62	731 ± 42
	200	0.16 ± 0.02	206 ± 21	2.25 ± 0.32	14.06 ± 0.92	729 ± 39
RyR3 (n = 9)	0	0.09 ± 0.02	16 ± 4	1.54 ± 0.77	17.11 ± 8.24	754 ± 27
	40	0.08 ± 0.03	18 ± 3	1.58 ± 0.31	19.75 ± 10.14	745 ± 19
	80	0.07 ± 0.01	21 ± 5	1.38 ± 0.49	19.71 ± 13.43	752 ± 30
	120	0.08 ± 0.02	18 ± 4	1.94 ± 0.71	24.25 ± 10.24	754 ± 28
	160	0.08 ± 0.01	20 ± 5	1.13 ± 0.02	14.15 ± 9.22	748 ± 32
	200	0.09 ± 0.02	18 ± 5	1.21 ± 1.22	13.44 ± 7.22	756 ± 36

Values shown are means ± SEM for $n \geq 9$ channels obtained from >3 separate preparations. *Denotes significantly different ($P < 0.05$) from that in absence of CCDI.

C2C12 cells with 75 and 100 μM CCDI, but the amplitude, time to peak and Ca^{2+} transient decay time were significantly smaller than those with 150 μM CCDI (data not shown). In medium without Ca^{2+}, CCDI (150 μM) also elicited a Ca^{2+} transient in C2C12 cells indicating that this drug mobilizes Ca^{2+} from internal Ca^{2+} stores [Figure 8B]. Mean Ca^{2+}-transient amplitude and decay time were similar to that seen with cells in Ca^{2+}-containing medium.

Addition of 100 μM ryanodine to C2C12 cells elicited a Ca^{2+} transient that lasted for about 20–30 s [Figure 8B(ii), upper panel]. Addition of CCDI (150 μM) to cells pre-exposed to ryanodine generated significantly reduced Ca^{2+} transients [$\Delta F = 0.3 \pm 0.1$ fluorescence units, Figure 8A(iii) and Figure 8B(○)].

CCDI did not mobilize Ca^{2+} from internal stores of rat primary ventricular myocytes

CCDI (150 μM) did not elicit Ca^{2+} transients in rat primary ventricular myocytes even after 500 s (Figure 9, also see Supporting Information Movie S2, CCDI on cardiac myocyte). Higher concentrations of CCDI were not used in this study. Addition of caffeine (10 mM) after addition of CCDI (~200 s), elicited a global rise in cytoplasmic Ca^{2+}, with amplitude of $\Delta F = 4.8 \pm 0.3$ fluorescence units, $n = 11$ cells Figure 9, consistent with our earlier reports (Shao *et al.*, 2007; 2009).

Discussion

In the present study, we describe the synthesis and chemical characterization of 2-cyclohexyl-3-cyclohexylimino-2,3-dihydro-pyrrolo[1,2-*c*]imidazol-1-one, (CCDI), a new ligand that preferentially modulates RyR1. This small molecule was obtained in good yields (~17%) by reacting pyrrole-2-carboxylic acid with DCC in carbon tetrachloride under reduced pressure (20 mmHg) and at 4°C. A similar yield for CCDI was also obtained using dichloromethane as the reaction solvent. No further attempts were made to increase the yield of CCDI by increasing either the amounts of starting reagents or the reaction solvent.

Although not soluble in water, CCDI is soluble in water-miscible organic solvents including ethanol, methanol and DMSO. Warming to 50°C also accelerated the dissolution of CCDI in these solvents. Dissolving CCDI in DMSO or ethanol first and then adding small amounts of warm water (50°C, 6:1 solvent : water ratio) retained up to 3 mg CCDI in solution mL^{-1} solvent : water mixture (~8–10 mM). However, when in water CCDI slowly hydrolyzed to form CPID (see Supporting Information Figure S3). Freeze-dried and crystalline CCDI stored in amber-coloured glass vials at room temperature and kept away from direct sunlight was stable for up to 2 years.

CCDI dose-dependently increased the binding of [^{3}H]-ryanodine to RyR1, but not to RyR2 or RyR3. The ability of

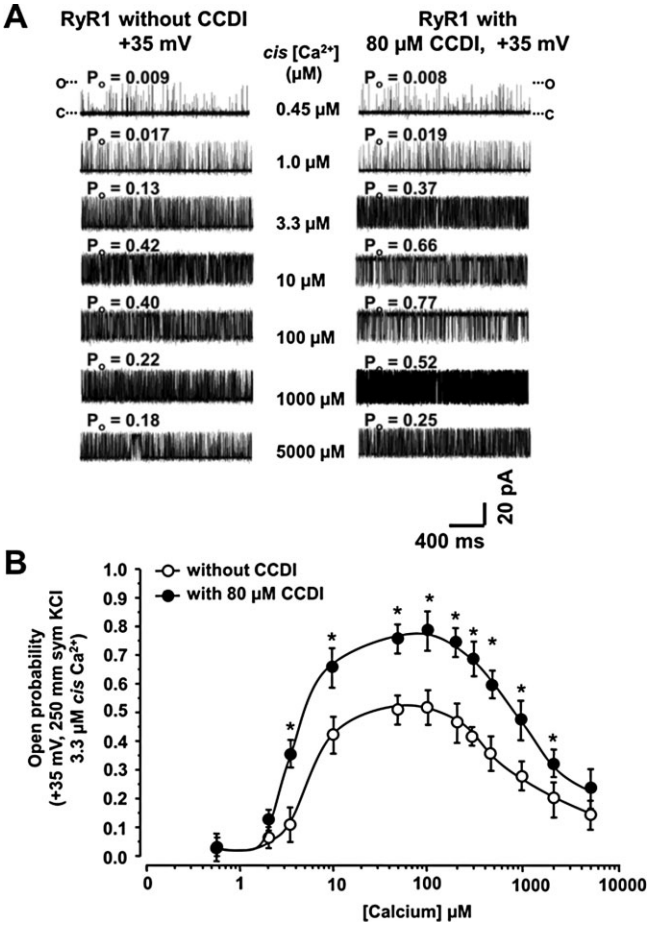

Figure 5

Effects of CCDI on the P_o of RyR1 at varying *cis* Ca^{2+}. (A) Representative 2 s recordings of RyR1 at +35 mV in the absence and presence of increasing amounts of *cis* Ca^{2+} with and without 80 μM CCDI. The graph in (B) shows mean ± SEM for n = 12 channels from two separate RyR1 preparations. *Denotes significantly different (P < 0.05) from that at the same Ca^{2+} concentration.

CCDI to potentiate [^{3}H]-ryanodine binding to RyR1 was not seen with buffer [Ca^{2+}] ≤5 or ≥2000 μM. However, at [Ca^{2+}] between 10 and 1000 μM, conditions that promoted the open state of the channel, CCDI increased the binding of [^{3}H]-ryanodine to RyR1. Similar trends were also seen in lipid bilayer assays. With [Ca^{2+}] of 0.45 and 1.0 μM, addition of 80 μM CCDI to the *cis* chamber did not significantly increase the P_o of RyR1. With *cis* [Ca^{2+}] between 3.3 and 2000 μM, addition of CCDI increased the P_o of RyR1. At 5000 μM *cis* Ca^{2+}, CCDI did not potentiate the P_o of RyR1. In an earlier study Copello *et al.* (1997) reported that a significant percentage of RyR1 in vesicular preparations were minimally responsive to *cis* Ca^{2+}. In this study, 3.3 μM *cis* Ca^{2+} was used for incorporation (and detection) of RyR1 in the bilayer. It is therefore likely that these conditions biased our data for channels that are Ca^{2+}-responsive. Nonetheless, when the P_os of the Ca^{2+}-responsive RyR1 were lowered to 0.02 using EGTA, CCDI was without effect. Although several ligands that modulate RyRs have been reported previously, including, ATP (Smith *et al.*, 1986, suramin (Emmick *et al.*, 1994), imperatoxins (Valdivia *et al.*, 1992) and chlorocresols (Choisy *et al.*, 1999; Fessenden *et al.*, 2003), to the best of our knowledge this is the first report on a ligand that preferentially modulates RyR1. Moreover, as the initial effect of CCDI (≤80 uM) was to increase the P_o of RyR1 by increasing the number of transitions from the closed to the opened state (Table 1), we reasoned that CCDI is binding to the closed state of RyR1 and increasing its sensitivity to Ca^{2+}, that is CCDI sensitizes RyR1 to Ca^{2+}. Whether CCDI also sensitizes RyR1 to other activator ligands including ATP and caffeine or blunts the ability of Mg^{2+} to inactivate RyR1 remains to be determined.

In this study we found that the effects of CCDI on RyR1 were reversible. Removing CCDI from the *cis* chamber by slow exchange of buffer (perfusion) returned the P_o of RyR1 to that which it was before the addition of *cis* CCDI. These data led us to conclude that the effects of CCDI on RyR1 resulted from its binding to a defined binding site(s) on RyR1, and not from covalent modifications (oxidization) of critical cysteine, methionine or other reactive residues (Xu *et al.*, 1998; Dulhunty *et al.*, 2000; Pessah and Feng, 2000). Although the location of the binding site for CCDI on RyR1 is not known at this time, several possibilities can be envisioned. Firstly, because CCDI altered the activity of RyR1 when added to the *cis* (cytoplasmic side), we reasoned that its binding site is located in the cytoplasmic domain of RyR1. Whether CCDI has binding site(s) on the luminal side of the channels remains to be validated. Secondly, the selectivity of CCDI for RyR1 suggests that its binding site could be located within a stretch of amino acids unique to RyR1. Sorrentino and Volpe (1993) earlier pointed out that although highly homologous, RyR1, RyR2 and RyR3 differed in their amino acid sequences in three distinct regions referred to as divergent region 1 (DR1 amino acids 4254–4631 for RyR1), divergent region 2 (DR2, amino acids 1342–1403 for RyR1) and divergent region 3 (DR3, amino acids 1872–1923 for RyR1). Available chimeras of RyR1/RyR2 and RyR1/RyR3 may be useful for deciphering which of these DRs CCDI is binding to. Thirdly, because low concentrations of CCDI increased the open probability of RyR1 by increasing the number of transitions from the closed to opened state, the binding site for CCDI could be located within or in proximity to the 'zipper-like structure' between amino acids 2000 and 2500 previously described by Ikemoto and Yamamoto (2002) or the region involved in the thermal stability of RyR1 (Yuchi *et al.*, 2012). Interactions with the 'zipper domain' could also help explain in part the ability of higher concentrations of CCDI to increase the mean open time of RyR1. Whether CCDI is interacting with more than one binding site on RyR1 remains to be determined. Fourthly, because the effects of CCDI on P_o were independent of the direction of the current flow (near identical effects seen at ±35 mV), we exclude the possibility that the binding site for CCDI is within the pore-forming region of RyR1.

In time-lapsed confocal studies, we found that the maximum Ca^{2+}-transient amplitude elicited by CCDI varied from cell to cell. These data probably reflect the varying quiescent states amongst C2C12 cells in culture. Quiescent cells with RyR1 in the low-activity state will probably be less

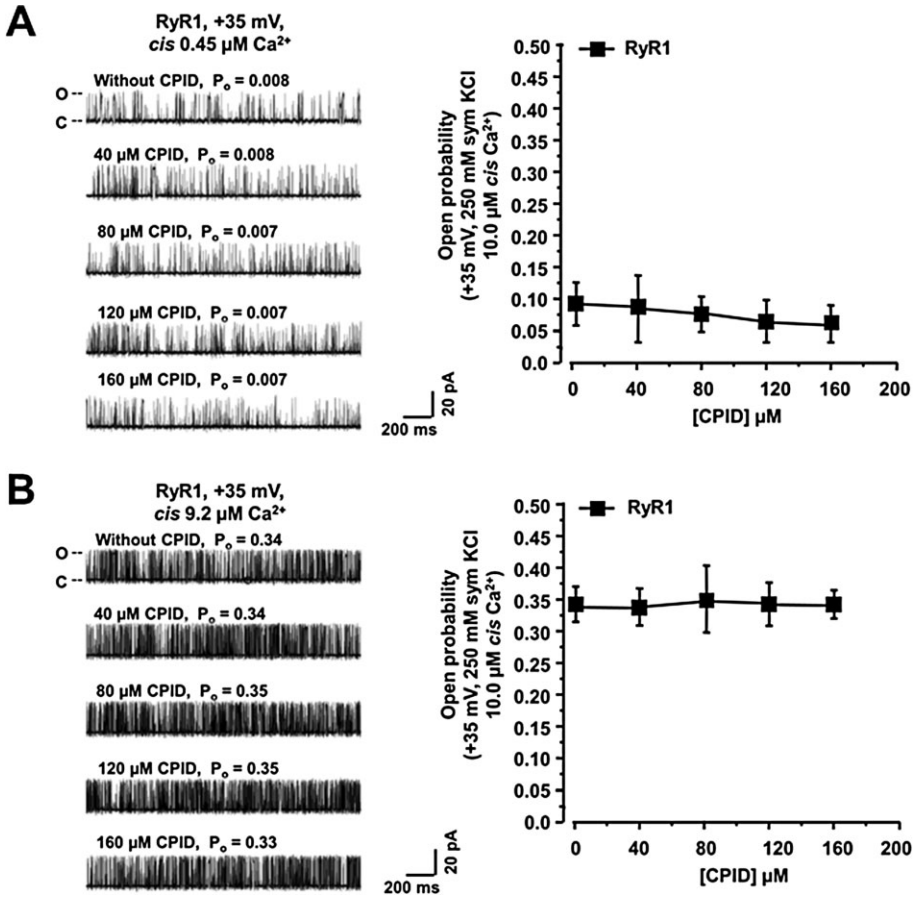

Figure 6

Effects of CPID on open probability (P_o) of RyR1 at 0.45 μM and 9.2 μM *cis* Ca^{2+}. (A) Left shows representative 2 s recordings of RyR1 at +35 mV with increasing amounts of CPID (0–160 μM) added to the *cis* chamber with 0.45 μM *cis* Ca^{2+} (low P_o channel). The graph in (A), right shows mean ± SEM for $n = 10$ channels from two separate RyR1 preparations. (B) Left shows representative 2 s recordings of RyR1 at +35 mV with increasing amounts of CPID added to the *cis* chamber with 9.2 μM *cis* Ca^{2+}. The graph in (B), right shows mean ± SEM for $n = 10$ channels from two separate RyR2 preparations.

responsive to CCDI, while non-quiescent cells with high-activity RyR1 will be more responsive to CCDI. We found that CCDI also elicited Ca^{2+} transients in C2C12 cells devoid of Ca^{2+} in the medium (data not shown), but not cells that were pretreated with ryanodine, emphasizing that this small-molecule ligand mobilizes Ca^{2+} from internal stores and via RyRs and not IP_3Rs, the other class of Ca^{2+} release channels in C2C12 cells (Grassi *et al.*, 1993; Bennett *et al.*, 1996). Although C2C12 cells also contain RyR3 (Bennett *et al.*, 1996; Powell *et al.*, 2001), it is unlikely that Ca^{2+} mobilization via RyR3 is a contributor to the Ca^{2+} transient, as CCDI displayed no effect on RyR3 *in vitro*.

In this study we found that CCDI hydrolyses in water, albeit slowly, to inactive CPID. The first evidence for this came when water was added at the end of the reaction; an estimated 5% of CCDI was hydrolysed to CPID. When left standing in DMSO : water (6:1) for 24 h, ~10% CCDI hydrolyses to CPID. While hydrolysis of CCDI in water to a biologically inactive substance is not a desired characteristic for a pharmaceutical, it is a desired feature in the design of chemicals to manage agricultural pests (Selby *et al.*, 2013), another area of research where extensive work on RyR ligands is being conducted. Formation of inactive metabolites with rain or during washing of agricultural produce in preparation for market significantly minimizes environmental and human toxicities. However, additional research is needed to investigate the potential of CCDI as a pesticide. For *in vitro* biological assays, we recommend dissolving CCDI in a water-miscible solvent such as DMSO or ethanol and use within 3–4 h of preparation.

In summary, this study has identified a small-molecule ligand, CCDI that preferentially binds to and activates mammalian RyR1. This new chemical entity did not significantly alter the function of mammalian RyR2 or RyR3, making it a useful research tool to delineate the physiological role(s) of RyR1 in cells with multiple RyR isoforms (e.g. smooth muscle cells). Although the ability of CCDI to hydrolyse in water may limit its usefulness in the development of human

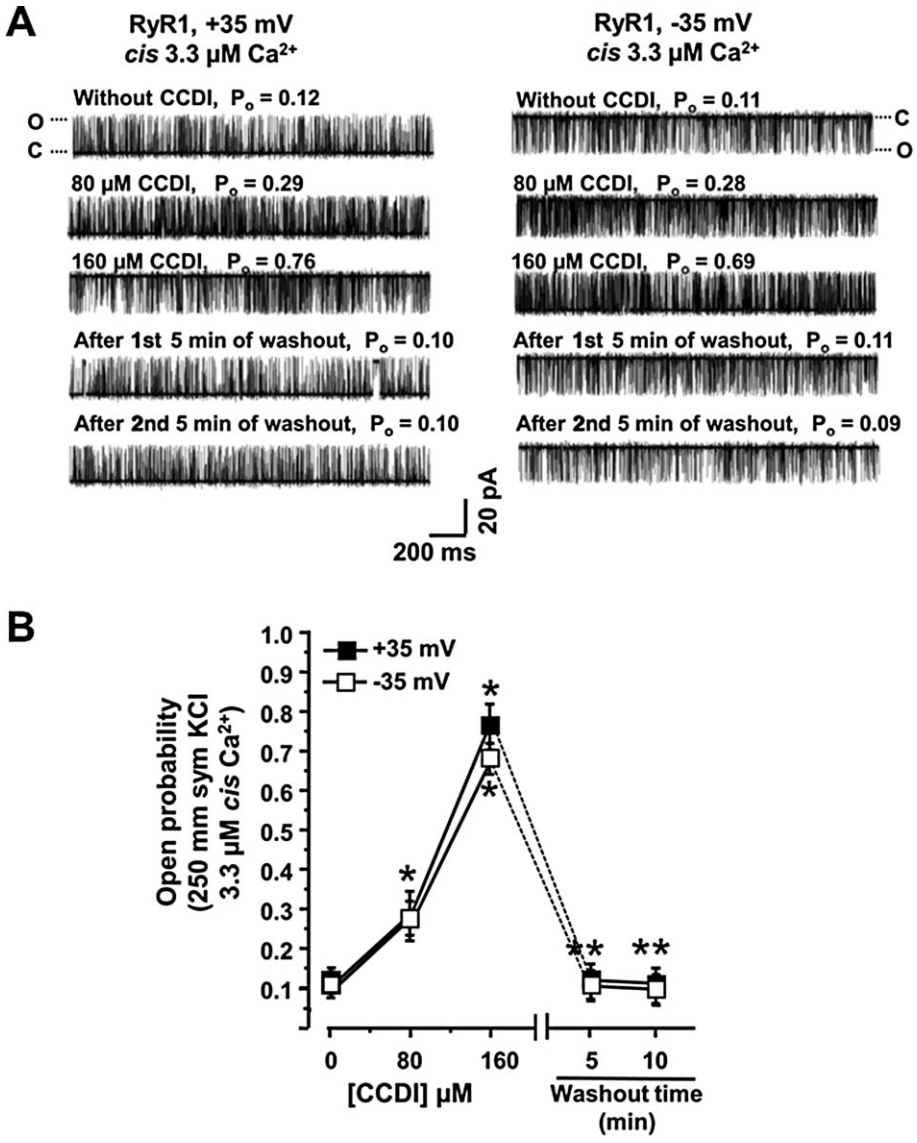

Figure 7

Graph showing the reversibility of actions of CCDI on RyR1. (A) Upper three left recordings show representative 2 s recordings of RyR1 at +35 mV with 3.3 μM Ca^{2+} and increasing amounts of CCDI (80 and 160 μM) added to the *cis* chamber. Upper three right recordings show representative 2 s recordings of RyR1 at +35 mV with 3.3 μM Ca^{2+} and increasing amounts of CCDI (80 and 160 μM) added to the *cis* chamber. Lower two recordings, left and right, show representative 2 s recordings of RyR1 5 and 10 min of washout at +35 and –35 mV respectively. (B) Shows mean ± SEM for $n = 6$ channels from two separate RyR2 preparations.

therapeutics, this drawback may be a desired property for the development of 'environmentally safe' pesticides.

Acknowledgements

We thank Dr. Gerhard Meissner and Xu Lu, University of North Carolina, Chapel Hill, NC for help with initial experiments, and Dr. Wayne S. R. Chen, University of Calgary, AB, Canada for providing cDNA encoding rabbit RyR3. The authors would also like to thank Drs. Amarnath Natarajan and Sandeep Rana, University of Nebraska Medical Center for critical discussions, The Eppley Structural Biology Core Facility, and Janice Taylor and James Talaska, University of Nebraska Medical Center, Confocal Core Facility for assistance. This work was funded in part by funds from the University of Nebraska Medical Center.

Authors contribution

C. T., C. H. S., C. P. and E. E., performed experiments, analysed data and/or edited the paper. S. K., J. S. and K. R. B came up with the idea, planed the experiments and edited the first

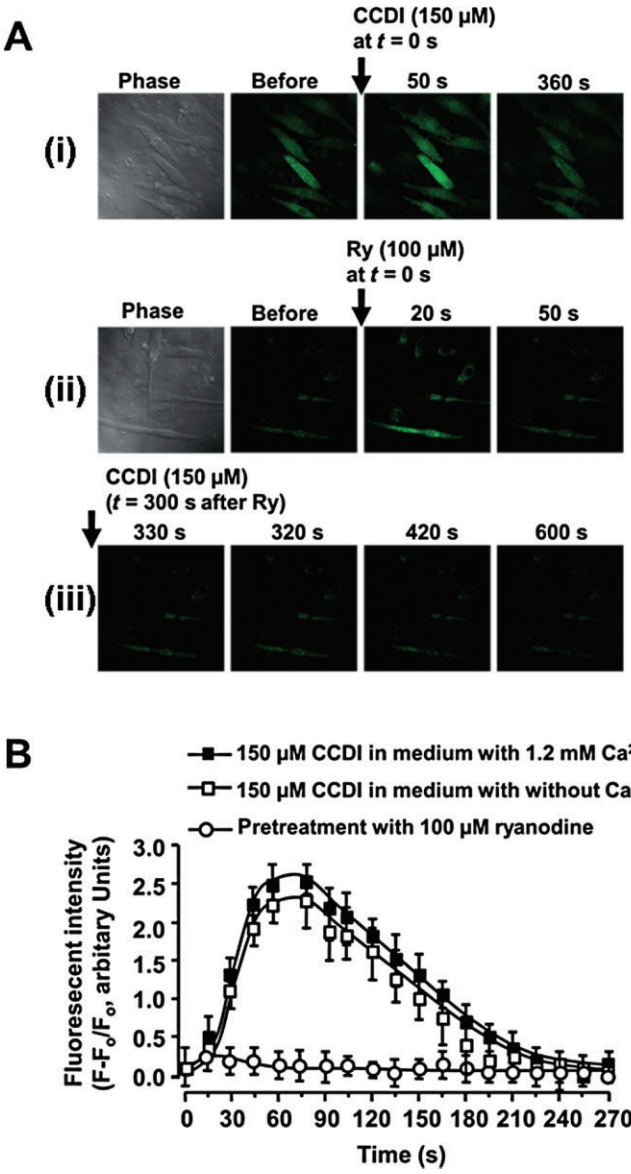

Figure 8

Ability of CCDI to mobilize Ca^{2+} from the internal stores of C2C12 cells. (A, i) Representative time-lapse confocal recording showing changes in intracellular Ca^{2+} in C2C12 cells in medium containing 1.2 mM Ca^{2+} challenged with 150 μM CCDI. (A, ii) Representative time-lapse recording of changes in intracellular Ca^{2+} of C2C12 cells in medium containing 1.2 mM Ca^{2+} challenged with 100 μM ryanodine. (A, iii) Representative time-lapse recording of changes in intracellular Ca^{2+} of C2C12 cells 5 min after pretreatment with 100 μM ryanodine. (B) Shows Ca^{2+} transients characteristics (mean ± SEM) from four chambers with n = 25 cells done on two separate days.

draft of the paper. C. T and K. R. B wrote the initial version ofthe paper.

Disclosures

None.

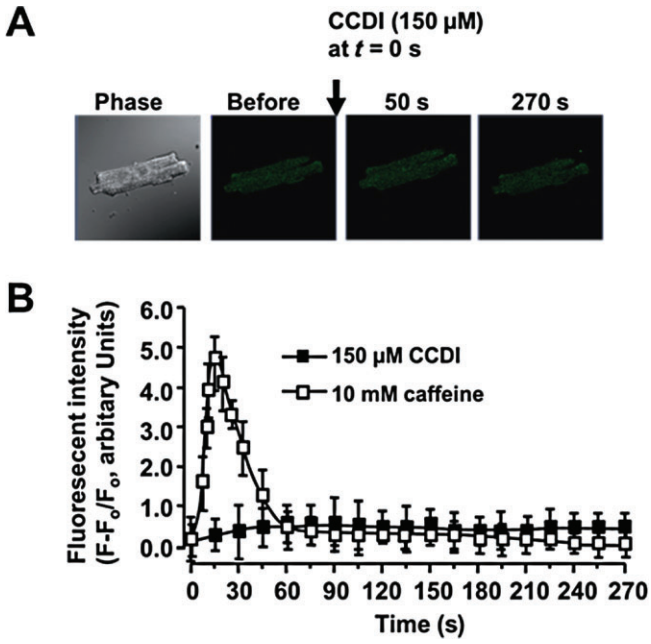

Figure 9

Ability of CCDI to mobilize Ca^{2+} from the internal stores of primary rat ventricular myocytes cells. (A) Shows a representative time-lapse confocal recording before and after addition of 150 μM to a rat primary ventricular myocyte in medium containing 1.2 mM Ca^{2+}. (B) Shows mean ± SEM for Ca^{2+} transients elicited by CCDI and caffeine (10 mM) from eight chambers with n = 11 rat ventricular myocytes.

References

Alexander SPH, Benson HE, Faccenda E, Pawson AJ, Sharman JL, Spedding M *et al.* and CGTP Collaborators (2013). The Concise Guide to PHARMACOLOGY 2013/14: G protein-coupled receptors. Br J Pharmacol 170: 1459–1581.

Bennett DL, Cheek TR, Berridge MJ, De Smedt H, Parys JB, Missiaen L *et al.* (1996). Expression and function of ryanodine receptors in non-excitable cells. J Biol Chem 271: 6356–6362.

Berridge MJ, Bootman MD, Roderick HL (2003). Calcium signalling: dynamics, homeostasis and remodelling. Nat Rev Mol Cell Biol 4: 517–529.

Bidasee KR, Besch HR Jr (1998). Structure–function relationships among ryanodine derivatives. Pyridyl ryanodine definitively separates activation potency from high affinity. J Biol Chem 273: 12176–12186.

Bidasee KR, Besch HR Jr, Kwon S, Emmick JT, Besch KT, Gerzon K *et al.* (1994). C_{10}-O_{eq}-N-(4-azido-5-^{125}iodo salicyloyl)-β-alanyl ryanodine (Az-βAR), a novel photo-affinity ligand for the ryanodine binding site. J Labelled Compd Radiopharm 34: 33–47.

Bidasee KR, Maxwell A, Reynolds WF, Patel V, Besch HR Jr (2000). Tectoridins modulate skeletal and cardiac muscle sarcoplasmic reticulum calcium-release channels. J Pharmacol Exp Ther 293: 1074–1083.

Bull R, Marengo JJ, Suárez-Isla BA, Donoso P, Sutko JL, Hidalgo C (1989). Activation of calcium channels in sarcoplasmic reticulum from frog muscle by nanomolar concentrations of ryanodine. Biophys J 56: 749–756.

Chen C, Okayama H (1997). High-efficiency transformation of mammalian cells by plasmid DNA. Mol Cell Biol 7: 2745–2752.

Choisy S, Huchet-Cadiou C, Leoty C (1999). Sarcoplasmic reticulum Ca^{2+} release by 4-chloro-m-cresol (4-CmC) in intact and chemically skinned ferret cardiac ventricular fibers. J Pharmacol Exp Ther 290: 578–586.

Conti A, Gorza L, Sorrentino V (1996). Differential distribution of ryanodine receptor type 3 (RyR3) gene product in mammalian skeletal muscles. Biochem J 316: 19–23.

Copello JA, Barg S, Onoue H, Fleischer S (1997). Heterogeneity of Ca^{2+} gating of skeletal muscle and cardiac ryanodine receptors. Biophys J 73: 141–156.

Cui L, Yang D, Yan X, Rui C, Wang Z, Yuan H (2013). Molecular cloning, characterization and expression profiling of a ryanodine receptor gene in Asian corn borer, *Ostrinia furnacalis* (Guenée). PLoS ONE 8: e75825.

Dulhunty A, Haarmann C, Green D, Hart J (2000). How many cysteine residues regulate ryanodine receptor channel activity? Antioxid Redox Signal 2: 27–34.

Emmick JT, Kwon S, Bidasee KR, Besch KT, Besch HR Jr (1994). Dual effects of suramin on calcium fluxes across sarcoplasmic reticulum membrane vesicles. J Pharmacol Exp Ther 269: 717–724.

Fessenden JD, Perez CF, Goth S, Pessah IN, Allen PD (2003). Identification of a key determinant of ryanodine receptor type 1 required for activation by 4-chloro-m-cresol. J Biol Chem 278: 28727–28735.

Futatsugi A, Kuwajima G, Mikoshiba K (1995). Tissue-specific and developmentally regulated alternative splicing in mouse skeletal muscle ryanodine receptor mRNA. Biochem J 305: 373–378.

George CH, Rogers SA, Bertrand BM, Tunwell RE, Thomas NL, Steele DS *et al.* (2007). Alternative splicing of ryanodine receptors modulates cardiomyocyte Ca^{2+} signaling and susceptibility to apoptosis. Circ Res 100: 874–883.

Giannini G, Conti A, Mammarella S, Scrobogna M, Sorrentino V (1995). The ryanodine receptor/calcium channel genes are widely and differentially expressed in murine brain and peripheral tissues. J Cell Biol 128: 893–904.

Grassi F, Giovannelli A, Fucile S, Eusebi F (1993). Activation of the nicotinic acetylcholine receptor mobilizes calcium from caffeine-insensitive stores in C2C12 mouse myotubes. Pflugers Arch 422: 591–598.

Hakamata Y, Nakai J, Takeshima H, Imoto K (1992). Primary structure and distribution of a novel ryanodine receptor/calcium release channel from rabbit brain. FEBS Letts 312: 229–235.

Ikemoto N, Yamamoto T (2002). Regulation of calcium release by interdomain interaction within ryanodine receptors. Front Biosci 7: d671–d683.

Jiang D, Xiao B, Li X, Chen SR (2003). Smooth muscle tissues express a major dominant negative splice variant of the type 3 Ca2+ release channel (ryanodine receptor). J Biol Chem 278: 4763–4769.

Kelliher M, Fastbom J, Cowburn RF, Bonkale W, Ohm TG, Ravid R *et al.* (1999). Alterations in the ryanodine receptor calcium release channel correlate with Alzheimer's disease neurofibrillary and beta-amyloid pathologies. Neuroscience 92: 499–513.

Lai FA, Liu QY, Xu L, el-Hashem A, Kramarcy NR, Sealock R *et al.* (1992). Amphibian ryanodine receptor isoforms are related to those of mammalian skeletal or cardiac muscle. Am J Physiol 263 (2 Pt 1): C365–C372.

Leeb T, Brenig B (1998). cDNA cloning and sequencing of the human ryanodine receptor type 3 (RyR3) reveals a novel alternative splice site in the RyR3 gene. FEBS Letts 423: 367–370.

MacKrill JJ (1999). Protein-protein interactions in intracellular Ca^{2+}-release channel function. Biochem J 337: 345–361.

MacLennan DH, Phillips MS (1992). Malignant hyperthermia. Science 256: 789–794.

Marks AR, Priori S, Memmi M, Kontula K, Laitinen PJ (2002). Involvement of the cardiac ryanodine receptor/calcium release channel in catecholaminergic polymorphic ventricular tachycardia. J Cell Physiol 190: 1–6.

McCarthy TV, Quane KA, Lynch PJ (2000). Ryanodine receptor mutations in malignant hyperthermia and central core disease. Hum Mutat 15: 410–417.

Neylon CB, Richards SM, Larsen MA, Agrotis A, Bobik A (1995). Multiple types of ryanodine receptor/Ca2+ release channels are expressed in vascular smooth muscle. Biochem Biophys Res Commun 215: 814–821.

Otsu K, Willard HF, Khanna VK, Zorzato F, Green NM, MacLennan DH (1990). Molecular cloning of cDNA encoding the Ca^{2+} release channel (ryanodine receptor) of rabbit cardiac muscle sarcoplasmic reticulum. J Biol Chem 265: 13472–13483.

Pessah IN, Feng W (2000). Functional role of hyperreactive sulfhydryl moieties within the ryanodine receptor complex. Antioxid Redox Signal 2: 17–25.

Powell JA, Carrasco MA, Adams DS, Drouet B, Rios J, Müller M *et al.* (2001). IP(3) receptor function and localization in myotubes: an unexplored Ca(2+) signaling pathway in skeletal muscle. J Cell Sci 114: 3673–3683.

Selby TP, Lahm GP, Stevenson TM, Hughes KA, Cordova D, Annan IB *et al.* (2013). Discovery of cyantraniliprole, a potent and selective anthranilic diamide ryanodine receptor activator with cross-spectrum insecticidal activity. Bioorg Med Chem Lett 23: 6341–6345.

Shao CH, Rozanski GJ, Patel KP, Bidasee KR (2007). Dyssynchronous (non-uniform) Ca^{2+} release in myocytes from streptozotocin-induced diabetic rats. J Mol Cell Cardio 42: 234–246.

Shao CH, Wehrens XH, Wyatt TA, Parbhu S, Rozanski GJ, Patel KP *et al.* (2009). Exercise training during diabetes attenuates cardiac ryanodine receptor dysregulation. J Appl Physiol 106: 1280–1292.

Shao CH, Tian C, Ouyang S, Moore C, Alomar F, Nemet I *et al.* (2012). Carbonylation induces heterogeneity in cardiac ryanodine receptors (RyR2) function during diabetes. Mol Pharmacol 82: 383–399.

Skeie GO, Romi F, Aarli JA, Bentsen PT, Gilhus NE (2003). Pathogenesis of myositis and myasthenia associated with titin and ryanodine receptor antibodies. Ann N Y Acad Sci 998: 343–350.

Smith JS, Coronado R, Meissner G (1986). Single channel measurements of the calcium release channel from skeletal muscle sarcoplasmic reticulum. Activation by Ca^{2+} and ATP and modulation by Mg^{2+}. J Gen Physiol 88: 573–588.

Sorrentino V, Volpe P (1993). Ryanodine receptors: how many, where and why? Trends Pharmacol Sci 14: 98–103.

Takeshima H, Nishimura S, Matsumoto T, Ishida H, Kangawa K, Minamino N *et al.* (1989). Primary structure and expression from complementary DNA of skeletal muscle ryanodine receptor. Nature 339: 439–445.

Takeshima H, Nishi M, Iwabe N, Miyata T, Hosoya T, Masai I *et al.* (1994). Isolation and characterization of a gene for a ryanodine receptor/calcium release channel in *Drosophila melanogaster*. FEBS Lett 337: 81–87.

Tian C, Shao CH, Fenster DS, Mixan M, Romberger DJ, Toews ML *et al*. (2010). Chloroform extract of hog barn dust modulates skeletal muscle ryanodine receptor calcium-release channel (RyR1). J Appl Physiol 109: 830–839.

Tian C, Shao CH, Moore CJ, Kutty S, Walseth T, DeSouza C *et al*. (2011). Gain of function of cardiac ryanodine receptor in a rat model of type 1 diabetes. Cardiovasc Res 91: 300–309.

Valdivia HH, Kirby MS, Lederer WJ, Coronado R (1992). Scorpion toxins targeted against the sarcoplasmic reticulum Ca(2+)-release channel of skeletal and cardiac muscle. Proc Natl Acad Sci USA 89: 12185–12189.

Xu L, Eu JP, Meissner G, Stamler JS (1998). Activation of the cardiac calcium release channel (ryanodine receptor) by poly-S-nitrosylation. Science 279: 234–237.

Yuchi Z, Lau K, Van Petegem F (2012). Disease mutations in the ryanodine receptor central region: crystal structures of a phosphorylation hot spot domain. Structure 220: 1201–1211.

Zorzato F, Fujii J, Otsu K, Phillips M, Green NM, Lai FA *et al*. (1990). Molecular cloning of cDNA encoding human and rabbit forms of the Ca^{2+} release channel (ryanodine receptor) of skeletal muscle sarcoplasmic reticulum. J Biol Chem 265: 2244–2256.

Supporting information

Additional Supporting Information may be found in the online version of this article at the publisher's web-site:

http://dx.doi.org/10.1111/bph.12764

Figure S1 ^{1}H NMR spectra of CCDI, (R1SA). Spectrum was performed on a Varian 500 MHz nuclear magnetic resonance spectrometer using TMS and deuterated chloroform as references.

Figure S2 ^{13}C NMR spectra of CCDI. Spectrum was performed on a Varian 500 MHz nuclear magnetic resonance spectrometer using TMS and deuterated chloroform as references.

Figure S3 Representative thin layer chromatograph showing slow hydrolysis of CCDI in water. For this 5 mg of CCDI was dissolved in 1 mL of DMSO and then 166 µL distilled ionized water was added. The solution was mixed and left overnight at room temperature and pressure. Aliquots of CCDI (10 µL) were spotted on a pre-coated thin layer plate with fluorescence indicator (Sigma Aldrich, Saint Louis, MI, USA) before addition of water and 24 h after addition of water. Plate was chromatographed on chloroform-saturated tank for 1 h and visualized using a Kodak EDAS 290 transilluminator (Thermo Fisher Scientific Inc., Waltham, MA, USA).

Movie S1 CCDI (150 µM) globally increased cytoplasmic Ca^{2+} in C2C12 cells. Mouse skeletal muscle myoblasts (C2C12 cells) grown on laminin-coated glass-bottomed chambers in DMEM containing 1.2 mM $CaCl_2$, supplemented with 2% FBS and antibiotics (100 units per mL penicillin, 100 $\mu g \cdot mL^{-1}$ streptomycin and 100 $\mu g \cdot mL^{-1}$ gentamicin, pH 7.3) were allowed to grow and differentiate (Tian *et al*., 2010). At 60–70% confluency, differentiated myotubes were loaded with Fluo 3-AM (5 µM, for 30 min at 37°C), washed and placed on the stage of a laser confocal microscope (Zeiss LSM 510 equipped with an Argon-Krypton Laser, 25 mW argon laser, 488 nm, 1% intensity; Plan-Apochromat 63×/1.4 oil lens, pinhole 128 µm, pixel time 1.28 µs, stack size 1024 × 1024 × 1). CCDI (150 µM) was then added to the chamber and time-lapse confocal microscopy was conducted to assess changes in intracellular Ca^{2+} (every 10 s for 5 min). Movie S1 was created by importing the time-lapsed images in LSM Zen Software (Thornwood, NJ, USA).

Movie S2 CCDI (150 µM) did not alter cytoplasmic Ca^{2+} in freshly isolated rat ventricular myocytes. Ventricular myocytes isolated from rat hearts were attached to laminin-coated glass coverslips by incubating for 1 h at 37°C in DMEM with F12 and 1.2 mM Ca^{2+} as described earlier (Shao *et al*., 2009). Attached cells were then loaded with Fluo-3 (5 µM) for 30 min at 37°C. Extracellular Fluo-3 was remove by washing and myocytes were placed on the stage of a laser confocal microscope (Zeiss Confocal LSM 510 confocal microscope equipped with an argon–krypton laser 25 mW argon laser, 5% intensity). CCDI (150 µM) was then added to a corner of the chamber and changes in intracellular Ca^{2+} was determined using time-lapse imaging (Tian *et al*., 2010). Images were taken every 2 s for 5 min. Movie S2 was created by importing the time-lapsed images in LSM Zen Software.